



Non-linear relationships between air temperature and river water quality revealed by a panel dataset of 276 Chinese cities

Check for updates

Kehan Liang^{1,5}, Litiao Hu^{1,5}, Zongwei Ma ^{1,2,3}, Shenyuan Huang^{1,4}, Miaomia Liu ^{1,3}, Wen Fang ^{1,3}, Jianxun Yang ^{1,3,4} & Jun Bi ^{1,2,3}

The impact of air temperature on water quality is typically mediated through its influence on water temperature, evaporation, and physicochemical processes. A comprehensive understanding of air temperature's effects on river pollution is imperative, particularly given rising water scarcity and the increasingly frequent extreme temperature events in China. Here, we employ the fixed effects model to estimate the effects of air temperature on river water quality and elucidate inverted U-shaped responses through 276 Chinese cities from 2014-2020. Our results demonstrate that both single-day high temperatures ($>37^{\circ}\text{C}$) and heatwaves (four consecutive days above 35°C) significantly increase river permanganate index (COD_{Mn}) concentration, worsening organic pollution. Additionally, these extreme temperature events contribute over 67% and 10% to quality-based water scarcity, presenting considerable challenges to water withdrawals in cities. Our findings necessitate incorporating temperature-related considerations into contemporary and prospective river governance, contributing to the development of targeted adaptation strategies and enhancing water resource management.

The exacerbation of water scarcity can be attributed to water pollution^{1,2}, which is a substantial concern, particularly in regions already facing water shortages³. The availability of clean water is a prominent determinant of the health and well-being of residents, as well as a crucial factor in socio-economic development^{4,5}. Nevertheless, the interaction between climate change and urbanization is currently intensifying challenges related to water scarcity in river systems^{6,7}. Temperature plays a pivotal role in regulating river ecosystem dynamics⁸, notably influencing water quality through the sequential regulation of water temperature, evapotranspiration, the utility of runoff, and the physicochemical-biological responses⁹. Additionally, an increase in temperature can enhance the frequency and duration of extreme heat events¹⁰, increasing the level of pollution in rivers⁹. This introduces a considerable degree of uncertainty in water quality management and challenges the achievement of the United Nations (UN) Sustainable Development Goals (SDGs) for clean water.

The impact of temperature on water quality is a cumulative and long-term phenomenon that demands particular attention in light of the current climate change. Under conventional temperature, the Intergovernmental Panel on Climate Change's Sixth Assessment Report explicitly indicates water quality degradation associated with increased water and surface air temperature¹¹. Extreme temperature during drought and heatwaves has been demonstrated to degrade water quality by reducing river runoff and affecting the rate of biogeochemical processes^{9,12-14}. Furthermore, previous studies have also confirmed the robust relationships between air temperature and water quality changes through specific watersheds^{15,16} and particular indicators¹⁷⁻¹⁹, providing a degree of qualitative insight. Despite extensive investigations and documentation of the effects of temperature on water quality, quantitative research covering multiple water quality indicators at the national city level and multiple time dimensions are still lacking.

¹State Key Laboratory of Water Pollution Control and Green Resource Recycling, School of the Environment, Nanjing University, Nanjing, China. ²Jiangsu Collaborative Innovation Center of Atmospheric Environment and Equipment Technology (CICAET), Nanjing University of Information Science & Technology, Nanjing, Jiangsu, China. ³Basic Science Center for Energy and Climate Change, Beijing, China. ⁴Institute for the Environment and Health, Nanjing University, Suzhou, China. ⁵These authors contributed equally: Kehan Liang, Litiao Hu. e-mail: zma@nju.edu.cn

China, the world's largest developing country with a large total population²⁰, however, possesses only a quarter of the global average per capita water availability²¹. The rapid economic development that has occurred in recent decades has inevitably resulted in the exacerbation of water pollution in cities, leading to water crises and diseases that threaten public health^{22,23}. The rivers of China are dominated by oxygen-consuming pollution, i.e., permanganate index (COD_{Mn}) and ammonia nitrogen (NH₃-N), and a series of corresponding discharge reduction targets have been established²⁴. Despite the achievements of water quality improvement through water pollution control actions in China, the distribution of water quality varies across the country². Furthermore, a seasonal trend in water quality is observed, with a notable decrease in dissolved oxygen (DO) and increases in COD_{Mn} and NH₃-N in most basins in summer^{2,25}. Moreover, surface air temperature in China is rising at a rate that exceeds the global average²⁶, necessitating urgent attention to temperature-induced alterations in water quality at the city level over extended time periods.

In this research, we employ fixed effects models to estimate the impacts of air temperatures (i.e., normal and high temperatures, and heatwaves) on water quality in 276 Chinese cities, and analyze heterogeneity by region and season (Fig. 1). To more accurately quantify the net effects of temperature on water quality, control variables such as gross regional product (GDP), amount of wastewater discharge, secondary production output share, and precipitation are included in the models. Furthermore, the contribution of temperature to quality-based water scarcity risks is calculated. The research enables the identification of risk-prone areas vulnerable to water quality degradation or notable water scarcity under the impacts of climate change, providing valuable insights into optimal climate risks and water management policies.

Results and Discussion

Effects of air temperature on water quality

Our findings reveal inverted U-shaped non-linear relationships between daily air temperature and concentrations of DO, COD_{Mn} and NH₃-N (Table 1), consistent with previous regional lake dataset validation or experimental and observational studies^{16,17,27,28}. Such consistency across different but related environmental contexts is probably because with rising temperatures, the decomposition of organic and inorganic substances initially lags behind the production, but eventually exceeds it²⁹. Consequently, the marginal effects of temperature shift from positive to negative, leading the total effects to first increase and then decline (Fig. 2). Specifically, the inflection points for the effects of temperature on DO, COD_{Mn}, and NH₃-N exhibit certain variations, being -4°C , -2°C , and -21°C , respectively (Fig. 2a, c, e). The continuous decline after the inflection threshold is probably caused by the increase in biodegradation activity under higher temperatures^{30,31}, which decomposes COD_{Mn} and NH₃-N in the river, while consuming oxygen. Furthermore, enhanced volatilization or adsorption of some organic compounds, as well as nitrification, denitrification, and volatilization³² at higher temperatures, contribute to the decreasing trend of COD_{Mn} and NH₃-N, respectively. In contrast, prior to the threshold, rising temperatures in the lower temperature range facilitate stream primary productivity^{17,33}, potentially increasing DO. While substrate release, solubility of organic compounds, and ammonification³⁴, release of macroinvertebrate excretions³⁵ with rising temperature promote the elevation of COD_{Mn} and NH₃-N. Interestingly, the total effects are negative while the marginal are positive for DO and COD_{Mn} at below -7°C and -4°C (Fig. 2b, d), respectively. Gas exchange hindered by ice on the river surface and the low activity of organic compounds at low temperatures may contribute to this result. However, the temperature thresholds in our study vary from previous work^{16,17,27,28}, likely due to differences in hydrology, temperature ranges, and methodology. In addition, biological treatment efficiency of wastewater pollutants before discharge is closely related to the temperature³⁶, which at high levels boosts microbial activity contributing to the removal efficiency.

Besides exploring on the daily scale, we further investigate the temperature impacts at longer time scales, including five, ten, and fifteen days and month (Table 2). The inverted U-shaped non-linear effects on DO and COD_{Mn} are enhanced at longer time scales in all cases (Fig. 2a-d), while NH₃-N is insignificant (Fig. 2e, f). The impacts in different municipalities

distribution also show a consistent trend across time scales (Supplementary Figs. 1-3). The results may be attributed to deeper dynamic processes and environmental changes under temperature variation at larger time scales³⁷, such as biological population turnover³⁸, metabolism³⁹, flow exchange³⁷, and water stratification⁴⁰. Nevertheless, the resilience of nitrogen microbial activity to short-term surface water exchange and changes in water composition⁴¹ may result in insignificant fluctuations with temperature changes. These findings emphasize the importance of different time scales for water management policy design, particularly in light of cumulative impacts of temperature at longer time scales, which are still concerning although currently less pronounced than rainfall or anthropogenic discharges^{42,43}, especially in global warming.

We further observe that the temperature and precipitation interactions are significantly positive in the models of DO and NH₃-N at the daily scale (Table 1 (1, 3)). As illustrated in Supplementary Fig. 4, at similar higher temperature levels, the concentrations of DO and COD_{Mn} in the river rise with increasing precipitation. This phenomenon may be attributed to the capacity of precipitation to transport large amounts of unconsumed oxygen and nutrient inputs into the river on a daily basis⁴⁴. Therefore, precipitation is also an indispensable factor in assessing climatic influences on water quality¹³ and should be taken into account when formulating climate change-related response strategies.

Impact heterogeneity of region

As shown in Supplementary Figs. 5 and 6, the Haihe River, as well as the middle and lower reaches of the Yellow River, are distinguished by exceptional water quality concerns, notable temperature fluctuations, and a considerable population density². Consequently, we have conducted a detailed examination of the pollutant indicators within this region, employing a differentiated approach. The findings indicate that the temperature effects in these regions are consistent with the main results, maintaining an inverted U-shape (Supplementary Fig. 7). Notably, in the $0 \sim 15^{\circ}\text{C}$ interval, the effect on COD_{Mn} still increases with rising temperatures, while at temperatures above 0°C , decreases in both COD_{Mn} and NH₃-N are less pronounced than in the national samples (Supplementary Fig. 7b, d). This underscores the necessity for targeted measures to address oxygen-depleting water pollution under temperature impact in areas with existing water quality issues.

Considering the regional variation in temperature distribution across China, we assess the spatial heterogeneity of temperature impacts (Fig. 3a, b). The data are categorized into four groups: northeastern, eastern, central, and western areas (Supplementary Fig. 8a). We find the quadratic term of temperature coefficients in northeastern region becomes greater than national samples, potentially related to the higher sensitivity of water bodies to temperature difference⁴⁵ and higher water quality bottom (Supplementary Fig. 6). In the eastern region, the effect of temperature on DO shifts to a negative effect. This is probably attributed to higher generation of anthropogenic pollutants from densely populated area⁴⁶ and low rate of slow-flowing gas exchange⁴⁷ caused by the small topographic drop (Supplementary Fig. 5). With more anthropogenic pollutants and low oxygen recharge, higher temperature increases oxygen consumption, resulting in declining DO. Temperature in the central and western regions significantly reduces NH₃-N, probably due to large changes in topography, with sufficient oxygen exchange, and enhanced activities of consuming NH₃-N microorganisms at higher temperatures.

We further investigate the heterogeneity in the Yangtze and Yellow River Basins (Supplementary Fig. 8b), indicating greater and more significant effects in Yangtze River basin than Yellow River basin (Fig. 3c, d). Specifically, the effects on DO and COD_{Mn} in Yangtze River Basin turn to negative effects. This can be attributed to the warmer and wetter climate in Yangtze River may enhance active chemical and biological behaviors and lead to more obvious water quality fluctuations.

Impact heterogeneity of season

The annual temperature distribution is characterized by distinct seasonal variations (Supplementary Fig. 9), and we further explore the impact of

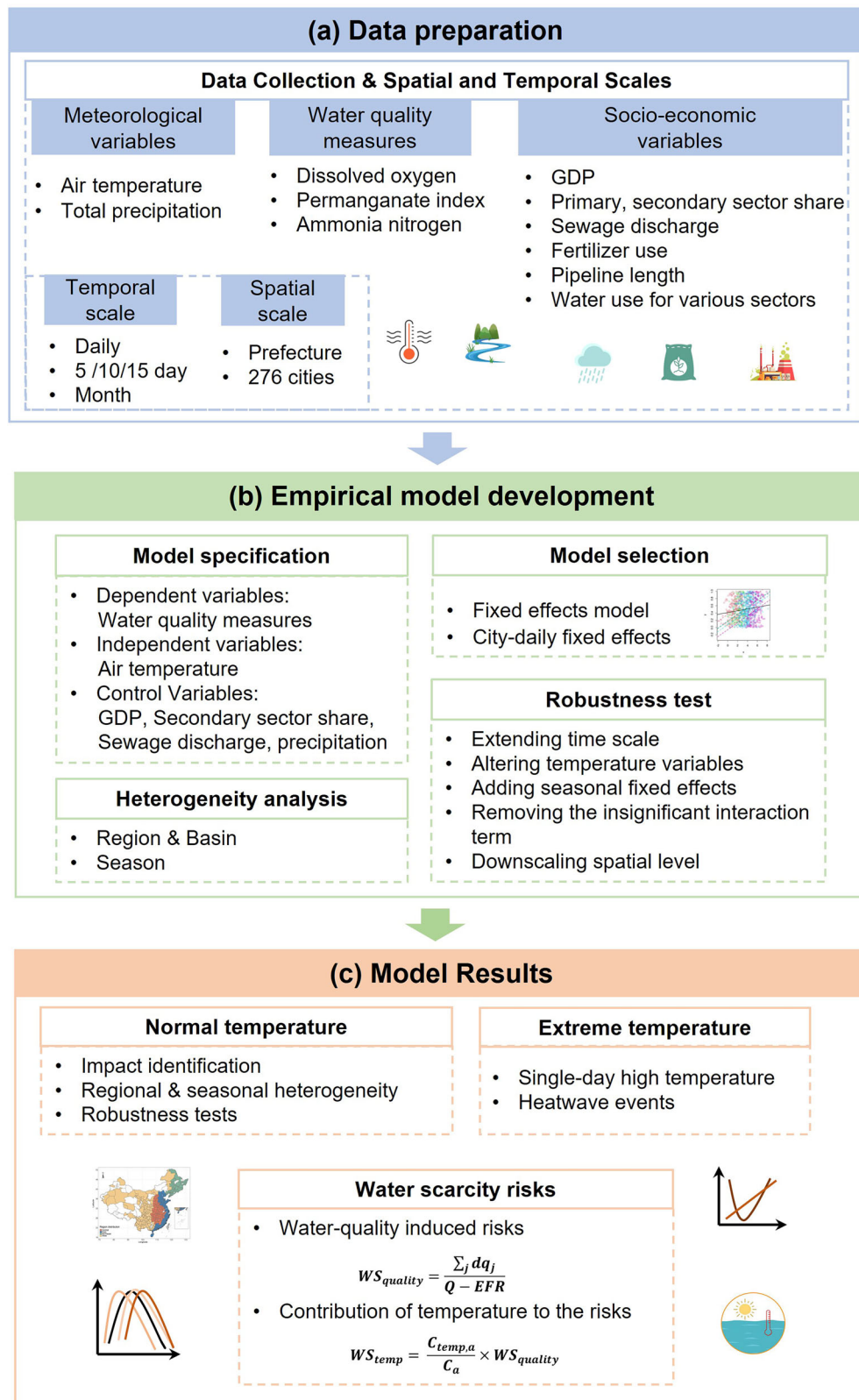


Fig. 1 | Flowchart of the research strategies. **a** Data preparation, including data collection and spatial and temporal scales; **b** Empirical model development, including data model specification, model selection, heterogeneity analysis,

robustness test, and spatial and temporal scales; **c** Model results, including normal temperature, extreme temperature, and water scarcity risks.

seasonal effects on water quality (Fig. 4). During summer, the influence on DO is predominantly negative and may be related to high water temperature within the season. In the other seasons, the effects reduce probably because of relatively flat temperature fluctuations, which serve to diminish the DO variations.

In winter, COD_{Mn} concentration increases with rising temperature, which can be attributed to weaker biological activity under colder water temperature, impeding the timely decomposition of organic pollutants⁴⁸. Additionally, lower runoff volume during winter ultimately leads to a higher

Table 1 | Panel regression results for the effects of daily average temperature

	(1) DO	(2) COD _{Mn}	(3) NH ₃ -N
Temp	−0.00177 (0.0017)	−0.000712 (0.0023)	−0.0141*** (0.0037)
Temp ²	−0.000238*** (0.000053)	−0.000197*** (0.00005)	−0.000332*** (0.00001)
Prec	−4.27*** (1.1)	−1.69 (1.8)	−9.11*** (2.7)
GDP	−0.000126* (0.000068)	0.0000671 (0.00034)	0.000368 (0.00056)
Industry	0.368 (0.23)	0.664 (0.78)	−0.0858 (0.72)
Emission	0.025 (0.018)	−0.0549 (0.06)	−0.071 (0.13)
Temp × Prec	0.119** (0.053)	0.0569 (0.078)	0.41*** (0.12)
N	170752	118489	135182
adj. R ²	0.436	0.593	0.475
BIC	54,451	141,826	314,283

Note: The coefficients are the regression results of the main models for DO, COD_{Mn}, and NH₃-N, representing the 100%-point effect on water quality per unit increase for a given temperature.

“Temp”, the daily air temperature; “Prec”, total daily precipitation; “GDP”, total GDP; “Industry”, the percentage of GDP output of the secondary sector; “Emission”, wastewater discharged; “N”, the number of observations. Standard errors are clustered at the municipal level and are shown in parenthesis.

* $p < 0.1$, ** $p < 0.05$, *** $p < 0.01$.

COD_{Mn} concentration. The inverted U-shaped effects are most pronounced in the spring and autumn, when temperature fluctuations are most noticeable, and they enhance the rates of dissolution and decomposition of water pollutants. The effects of temperature on NH₃-N are significant mainly in spring and autumn, with a significant linear negative pattern in spring and an enhanced inverted U-shaped response in autumn. This may be related to the relatively higher temperature in spring and autumn, increasing the vitality of biological activities⁴⁹.

Robustness tests

We conduct several robustness tests to verify the observed effects of air temperature on water quality. We first expand the time scale of the data to the seasonal scale to ensure the suitability of the model at a larger time scale to validate the main model of this study (Supplementary Table 3). Secondly, we replace the independent variables with daily maximum and minimum temperature on the daily scale model to ensure the wide application and prevent the contingency of the independent variables (Supplementary Table 4). Thirdly, we introduce seasonal fixed effects to control for seasonal disturbances in water quality, further testing the robustness of time fixed effects (Supplementary Table 5). Fourthly, we determine robustness to remove the insignificant interaction term between precipitation and temperature on the monthly scale (Supplementary Table 6). Finally, we validate our main findings by downscaling the data to the monitoring section level, thereby confirming the model’s applicability at a finer spatial scale (Supplementary Table 7). Across these tests, the effects of temperature are consistent with the results of the main model, indicating the robustness of the model in this study.

Results of extreme heat temperature

The quality of water subjected to elevated temperatures for extended periods may undergo substantial alterations from its typical patterns, potentially resulting in long-term deterioration⁵⁰. We apply the daily maximum temperature above 35 °C to explore the effects of extreme temperature. It is

notable that the response of COD_{Mn} shifts to a positive U-shape and subsequently increases above 37 °C, suggesting high temperature can contribute to the deterioration of water quality (Supplementary Table 8 and Fig. 5). This is associated with reduced stream flow⁹, a higher solubility of organic matter⁵¹, and inhibition or inactivation of biological enzymes involved in the degradation of organic compounds^{52,53} under high temperature conditions. High temperature has little effect on DO and NH₃-N, potentially because of the low levels of DO in the river and the limitation of conversion reactions associated with NH₃-N in high temperature interval⁵⁴.

Furthermore, an investigation into the effects of heatwaves is conducted based on a single day of high temperatures exceeding 35 °C, with the duration of the heatwaves lasting for two, three, and four days (Supplementary Table 9). The effect of extreme high temperature on COD_{Mn} is significant and exhibits a positive U-shaped relationship across the three scenarios. When exceeding 35 °C for two and four consecutive days, the concentration of COD_{Mn} increases by 9% and 10%, respectively. Rapid algal and phytoplankton blooms and metabolic die-offs under continuous high temperatures may result in higher organic matter concentrations⁹. Although DO and NH₃-N show weak responses under extreme temperatures, other parameters such as salinity, algae, and nutrients are also often highly correlated with COD_{Mn}^{55–57}. Consequently, these indicators are likely to exhibit elevated concentration, and patterns have been demonstrated in previous studies^{9,14}. Therefore, it is necessary to further confirm the effects of extreme temperature scenarios with available water quality data in the future, proposing strategies to strengthen ecosystem resilience and adaptive management for high-temperature stress.

Quality-based water scarcity risks under extreme temperatures

As illustrated in *Section Results of extreme heat temperature*, the occurrence of extreme temperatures has been observed to result in an increase in COD_{Mn} concentrations, thereby further exacerbating the risk of water scarcity driven by temperature under local water pollution risks (Supplementary Note 1 and Supplementary Fig. 10). We screen the samples with increased concentration caused by extreme temperatures and calculate total water scarcity risk induced by COD_{Mn} (Eq. (5)). Most of the municipalities in the sample (such as Hangzhou and Nanchang cities) are not at risk of quality-based water scarcity under extreme temperature, but we also capture areas that are relatively highly affected (Fig. 6). For single-day high temperature, cities such as Jiaxing, Zhumadian, Shangqiu, Zhoukou, Fuyang, Hefei, and Wuhu are exposed to COD_{Mn}-induced quality-based water scarcity risks, with the contribution of temperature exceeding 67% (i.e., the contribution of temperature to COD_{Mn}-induced risk (Eq. (6)) divided by total COD_{Mn}-induced risk (Eq. (5))) (Fig. 6a). The heat wave scenario (four consecutive days above 35 °C) is essentially similar to the high temperature scenario, with the highest risk of water scarcity in Huabei, followed by Shangqiu, which face additional water scarcity risk of 0.12 and 0.02 (WS_{quality-hw}), respectively (Fig. 6b). This means that the heatwave-driven elevation of COD_{Mn} requires the city to obtain additional 12% and 2% of available water withdrawals, respectively, to satisfy the water demand of the sector. Therefore, despite the relatively small number of risk samples captured currently, the potential contribution to quality-based water scarcity risk in future scenarios with extreme temperature events cannot be ignored. Our findings show a city is at water scarcity risk while the surroundings are not, which may be attributed to the low multi-year city’s water quality baseline (Supplementary Fig. 6). Furthermore, the results are also affected by the limitations posed by the absence of municipal water use data, which represents a challenge for subsequent studies to overcome.

Conclusion

Our findings quantify the impacts of air temperature on water quality, thereby providing valuable insights for decision makers to design evidence-based strategies regarding the management of river environments in climate change mitigation under current scenarios. This study is, to the best of our knowledge, the first to analyze the contemporary responses of Chinese

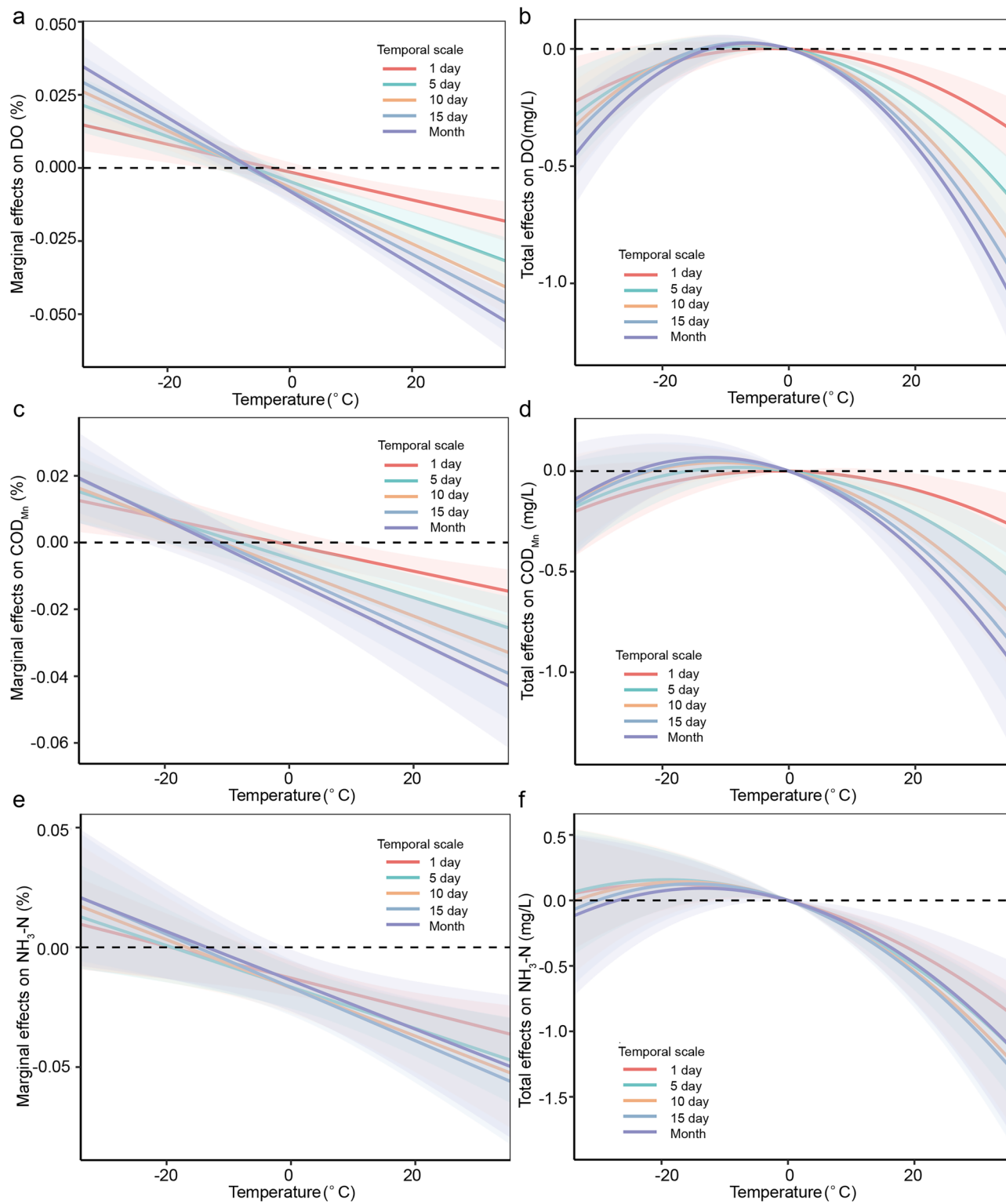


Fig. 2 | Marginal and total effects of temperature on water quality indicators at different time scales. **a** Marginal and **b** total effects of temperature on DO; **c** Marginal and **d** total effects of temperature on COD_{Mn}; **e** Marginal and **f** total effects of temperature on NH₃-N. The lines represent the nonlinear responses of three water quality indicators to temperature in the study region from 2014 to 2020, evaluated at

different temporal scales (colors). The effects were estimated according to Eq. (1). The marginal effects first increase above zero and then decline, while the total effects exhibit an inverted U-shaped response. The shaded areas around the curves indicate the 90% confidence intervals of the estimated temperature effects, with standard errors clustered at the city level.

municipal river water quality to temperature at a national scale and integrates with quality-based water scarcity assessment to yield three critical findings. Firstly, DO, COD_{Mn}, and NH₃-N exhibit inverted U-shaped responses to air temperature across various time scales (i.e., day, 5-day, 10-

day, 15-day, and month), with impacts gradually expanding with the larger time scales. Secondly, temperatures above 37°C for a single day and heat-waves exceeding 35°C for two and four consecutive days can significantly elevate COD_{Mn} concentrations in rivers. Finally, an increase in COD_{Mn}

Table 2 | Panel regression results of the main models in different temporal scales

	(1) DO	(2) DO	(3) DO	(4) DO	(5) COD _{Mn}	(6) COD _{Mn}
Temp	−0.00551*** (0.0019)	−0.00775*** (0.002)	−0.00931*** (0.0019)	−0.0103*** (0.0019)	−0.0047* (0.0028)	−0.00777*** (0.003)
Temp ²	−0.000385*** (0.000059)	−0.000483*** (0.000062)	−0.000546*** (0.000064)	−0.00063*** (0.00007)	−0.000295*** (0.000056)	−0.000356*** (0.000062)
Prec	−2.14*** (0.63)	−1.45*** (0.45)	−1.29*** (0.38)	−0.779*** (0.28)	−0.253 (0.99)	0.541 (0.71)
GDP	−0.000134* (0.000071)	−0.000134* (0.000073)	−0.000131* (0.000074)	−0.000131* (0.000077)	0.0000866 (0.00037)	0.000134 (0.00038)
Industry	0.376* (0.22)	0.314 (0.22)	0.291 (0.22)	0.223 (0.22)	0.646 (0.85)	0.584 (0.84)
Emission	0.0277 (0.019)	0.0299 (0.02)	0.0302 (0.02)	0.0331 (0.022)	−0.0412 (0.065)	−0.0319 (0.068)
Temp × Prec	0.0559** (0.028)	0.0362* (0.02)	0.0349** (0.016)	0.0243** (0.012)	0.0179 (0.044)	−0.0187 (0.032)
N	36243	18790	12866	6803	25557	13448
adj. R ²	0.465	0.475	0.474	0.482	0.601	0.605
BIC	6474	2232	1421	402	30512	15,826
Time Fixed Effect	5 day	10 day	15 day	Month	5 day	10 day
	(7) COD _{Mn}	(8) COD _{Mn}	(9) NH ₃ -N	(10) NH ₃ -N	(11) NH ₃ -N	(12) NH ₃ -N
Temp	−0.00942*** (0.0032)	−0.0111*** (0.0038)	−0.0165*** (0.0046)	−0.0169*** (0.0054)	−0.0168*** (0.0059)	−0.0138** (0.0066)
Temp ²	−0.000421*** (0.000076)	−0.00045*** (0.00011)	−0.000433*** (0.00013)	−0.000503*** (0.00016)	−0.000556*** (0.00018)	−0.00051*** (0.00019)
Prec	0.254 (0.78)	0.506 (0.47)	−1.34 (1.6)	−1.05 (1.3)	−0.137 (1.1)	0.482 (0.84)
GDP	0.000136 (0.00038)	0.000252 (0.0004)	0.000483 (0.00067)	0.000542 (0.00076)	0.000586 (0.00078)	0.000687 (0.00084)
Industry	0.616 (0.85)	0.428 (0.84)	−0.262 (0.81)	−0.398 (0.89)	−0.471 (0.92)	−0.6 (1)
Emission	−0.0366 (0.064)	−0.043 (0.066)	−0.0832 (0.14)	−0.0838 (0.15)	−0.0842 (0.15)	−0.096 (.16)
Temp×Prec	−0.00522 (0.033)	−0.0161 (0.02)	0.105 (0.066)	0.0789 (0.054)	0.0412 (0.048)	0.00506 (0.035)
N	9312	5037	29846	15860	11108	6123
adj. R ²	0.602	0.607	0.461	0.461	0.471	0.495
BIC	11,005	5680	69,074	36,896	26,199	14,688
Time Fixed Effect	15 day	Month	5 day	10 day	15 day	Month

Note: The coefficients are the regression results of the main models for DO, COD_{Mn}, and NH₃-N, representing the 100%-point effect on water quality per unit increase for a given temperature. "Temp", the air temperature; "Prec", total precipitation; "GDP", total GDP; "Industry", the percentage of GDP output of the secondary sector; "Emission", wastewater discharged; "N", the number of observations. Standard errors are clustered at the municipal level and are shown in parenthesis.

($p < 0.1$, $^*p < 0.05$, $^{**}p < 0.01$).

induced by single-day high temperature and heatwaves contributes to the quality-based water scarcity related to COD_{Mn} at a high level, with above 67% and 10%, respectively.

This work also highlights key hotspots and provides policymakers with temperature-related baseline insights for optimizing water quality management strategies. In southern China, rising temperatures have a more pronounced negative impact on DO. Regions with poor water quality, as well as the Northeast and the Yangtze River Basin, are particularly vulnerable to the adverse effects of normal temperature. To ensure the long-term sustainability of river ecosystems under rising temperatures, it is imperative to enhance the efficiency of water quality monitoring and governance through more effective

pollutant control, adaptive water management, and risk mitigation strategies. Cities such as Shangqiu, Huaipei and Wuhu should emphasize the contribution of temperature to the risk of quality-based water scarcity, and make timely adjustments to water withdrawals to guarantee the smooth operation of production and living conditions. Therefore, empirically-based national-scale impact identification and prediction are essential to inform policies aimed at achieving sustainable development. However, this study did not incorporate interactions between surface water and groundwater, the mediation effects among water quality indicators, or potential estimation biases arising from uncertain water withdrawal locations, which could be further examined in subsequent studies.

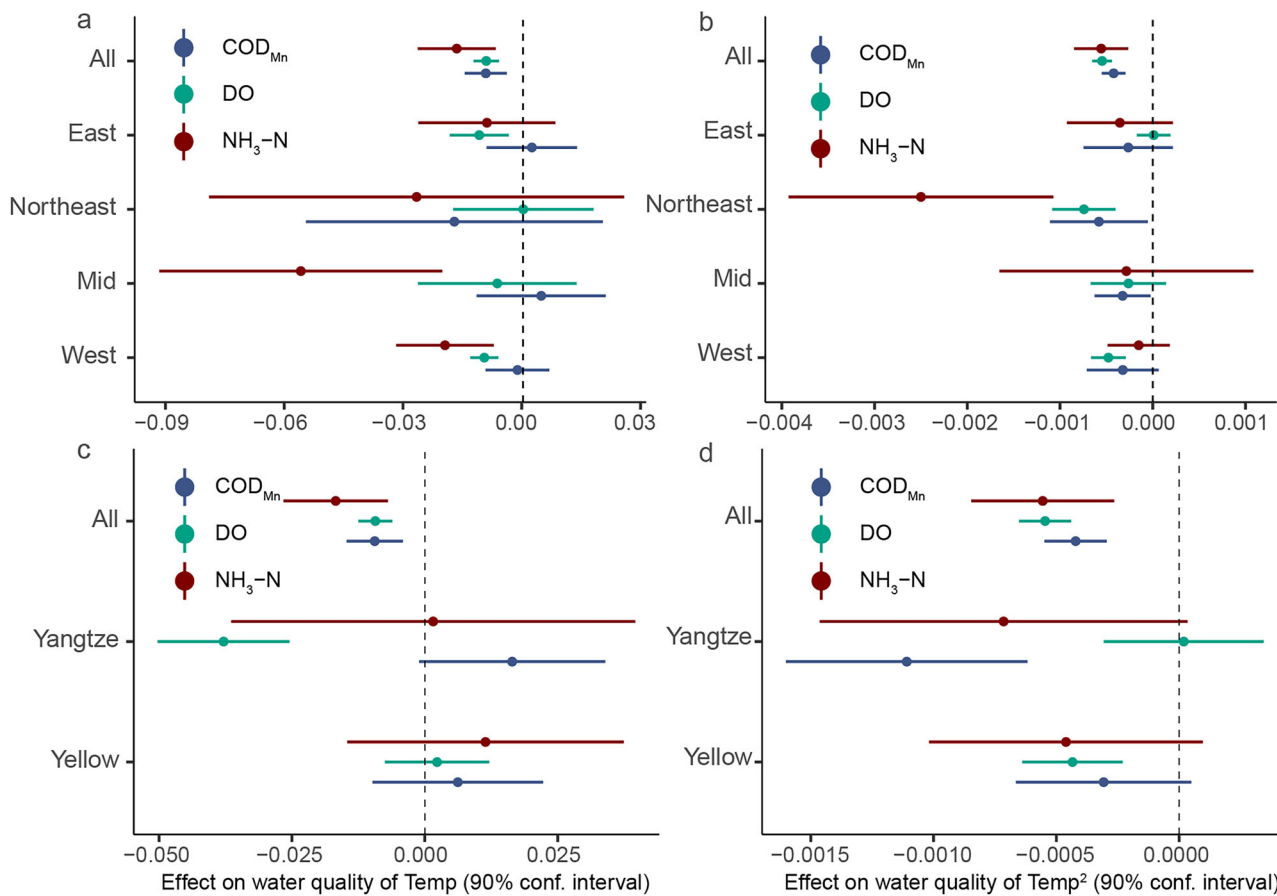


Fig. 3 | Regional heterogeneity analysis of temperature impacts on water quality at 15-day scales. Estimates of the effects of the **a** linear and **b** quadratic terms of temperature when dividing the data according to geographic distribution. Estimates of the effects of the **c** linear and **d** quadratic terms of temperature when dividing the data according to the Yangtze and Yellow Rivers. The point estimates show the

average effects of temperature under different groups, and the error bars represent the 90% confidence interval of the effect. The effects are estimated based on Eq. (1). The estimates reflect how water quality in each region responds to temperature according to the regional classification.

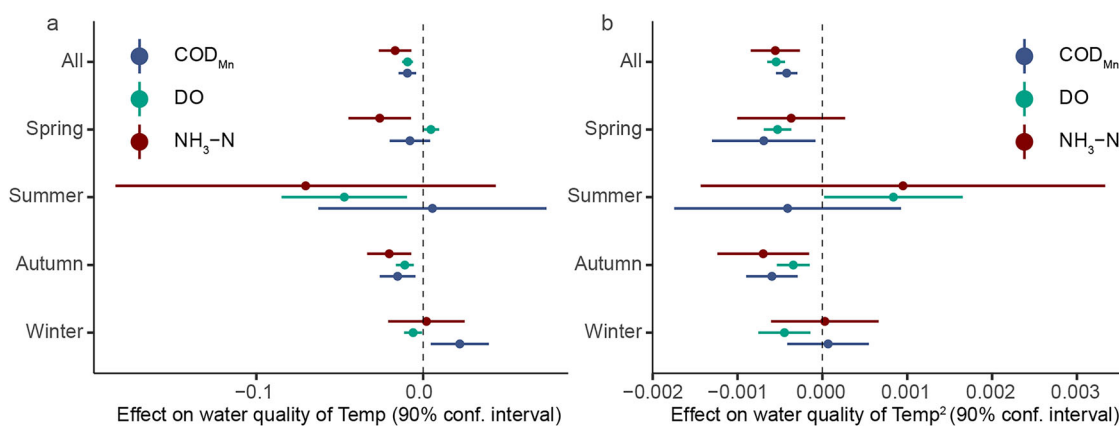


Fig. 4 | Seasonal heterogeneity analysis of temperature impacts on water quality at 15-day scales. **a** Estimates of impacts by the temperature linear term and **b** quadratic term when dividing the data by season. The point estimates show the

the 90% confidence interval of the effect. The effects were estimated based on Eq. (1). The estimates reflect how water quality in each season responds to temperature according to the seasonal classification.

Methods

Climate data

The meteorological data used in this study is the fifth generation ECMWF atmospheric reanalysis of the global climate (ERA5) reanalysis dataset⁵⁸. We use daily 2-meter mean air temperature for the 2014–2020 historical period, with total daily precipitation as a control variable. The data are collected at

0.25° × 0.25° grid on the daily scale, and are spatially merged according to the boundaries of municipalities to reflect the city temperature levels. To capture the effects' variations of different time scales, we merge the data at the five-day, ten-day, fifteen-day, and monthly scales. We also include daily maximum temperatures in the study to further analyze the impacts of extreme temperatures.

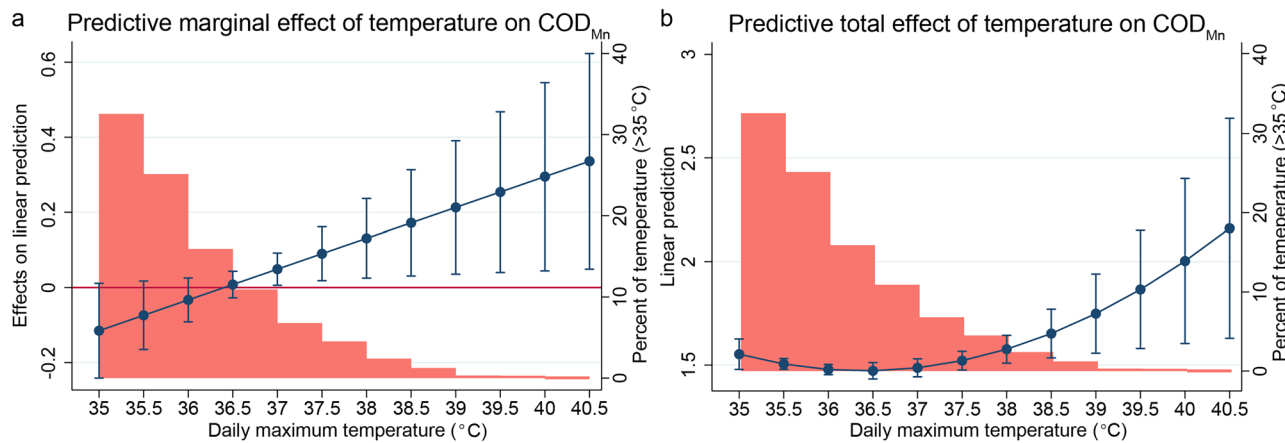


Fig. 5 | Effects of single-day high temperature on COD_{Mn}. **a** Marginal and **b** total effects of single-day high temperature on COD_{Mn}. The lines represent the nonlinear response of COD_{Mn} to temperature in the study area from 2014 to 2020. The effects were estimated based on Eq. (1). The marginal effect is initially negative and then becomes positive, while the total effect exhibits a U-shaped pattern. The starting and

ending points of each curve correspond to the historical range of daily maximum temperatures above 35 °C across all cities from 2014 to 2020. The shaded area around each curve represents the 90% confidence interval of the estimated temperature effect, with standard errors clustered by city. Full regression results are shown in Supplementary Table 8.

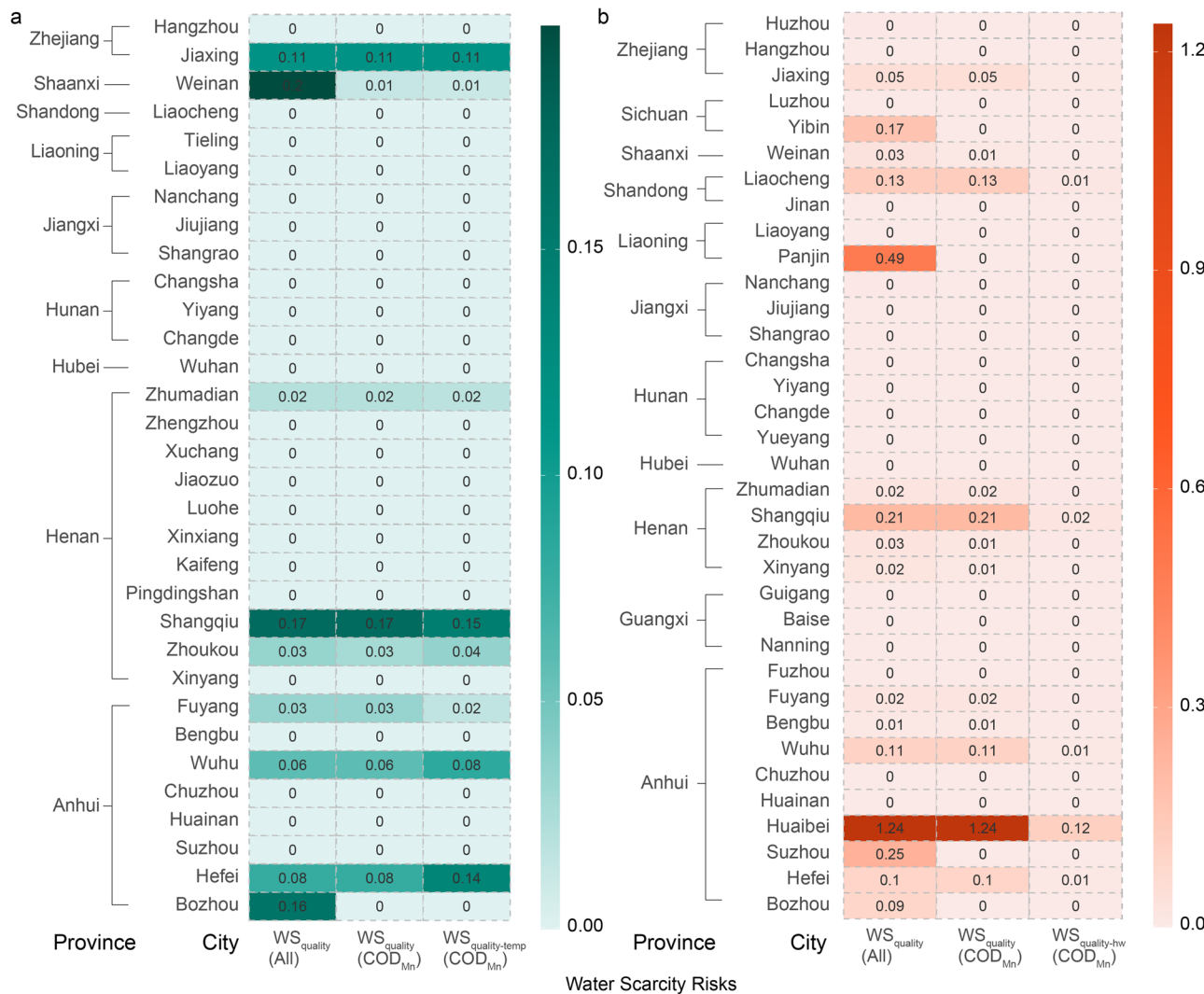


Fig. 6 | Water scarcity risks induced by water quality of city for high-temperature and heat wave of COD_{Mn} samples. **a** Risks for single-day high-temperature city samples. **b** Risks for heat wave city samples. WS_{quality} (All) refers to quality-based water scarcity induced by COD_{Mn} and NH₃-N, and WS_{quality} (COD_{Mn}) refers to quality-based water scarcity induced by COD_{Mn}. WS_{quality-temp} (COD_{Mn}) represents

the contribution of temperature to quality-based water scarcity induced by COD_{Mn}. WS_{quality-hw} (COD_{Mn}) represents the contribution of heatwave to quality-based water scarcity induced by COD_{Mn}. A scarcity risk value represents the proportion of additional water withdrawals required when water quality degradation under extreme temperature renders part of the sectoral water supply inapplicable.

We use precipitation as a control variable because it can form surface runoff, flushing pollutants from construction land and farmland into the water bodies⁴³. Moreover, under climate change, temperature and rainfall are strongly correlated, and changes in temperature tend to alter rainfall⁵⁹. Thus, to further understand the interactive effects of meteorological features on water quality, we include the interaction between temperature and precipitation. Descriptions of study area and the main variables are specified in the Supplementary Note 2 and Supplementary Figs. 6 and 11.

Water quality data

DO, COD_{Mn}, and NH₃-N are the main water quality indicators employed in this study. DO serves as a critical indicator of aquatic ecosystem functioning, reflecting biogeochemical processes including biological respiration and photosynthesis in water bodies¹⁷. COD_{Mn} represents the level of reducing organic pollution caused by eutrophication in aquatic systems⁶⁰. NH₃-N is one of the most important indicators for evaluating nitrogen pollution in water bodies, which also reflects the level of eutrophication⁶¹. The water quality data is obtained from the National Environmental Monitoring Centre of China (<http://www.cnemc.cn/ssj/>) in the form of 4-hourly cross-sectional monitoring data and combined by applying the arithmetic mean from each monitoring station across the city^{62,63}. Descriptions of the distribution of multi-year water quality conditions are specified in the Supplementary Note 3 and Supplementary Figs. 6 and 12.

Socio-economic data

Given that river water quality and climate conditions are both influenced by human activities, we select various socio-economic variables as control variables, and the descriptions of impacts are specified in Supplementary Note 4. To ascertain the net effects of temperature on water quality, a number of variables are obtained from the China Urban Statistical Yearbook. These include GDP of each industry, wastewater discharge (including domestic and industrial wastewater), nitrogen fertilizer application, and pipeline lengths.

Additionally, inadequate water quality can pose a critical constraint on water availability². In order to assess the quality-based water scarcity, data on agricultural, industrial, and domestic water usage in prefecture-level cities is collected from provincial water resources bulletins. Total water resources data is obtained from the Statistical Yearbook of China. Nevertheless, the data are insufficient in quantities due to the disparate publication of provincial documents, varying statistical formats, and the loss of documents in the bulletins. Thus, to reflect the national situation, we also collect data on water use and total water resources from the annual China Water Resources Bulletin at the provincial level.

Main models

We employ fixed effects panel regression models to estimate the effects of air temperature on water quality. The models, including city and time (i.e., day, 5-day, 10-day, 15-day, and month) fixed effects, can be effectively applied to strengthen causal effects assessment by adjusting for unobserved unit-specific and time-specific confounders^{64,65}. The main model specification of this study is shown in Eq. (1), involving the primary and quadratic terms of temperature, the interaction term between temperature and precipitation, and various control variables. We logarithmize the water quality indicators because of their highly skewed distribution (Supplementary Fig. 13). The t-statistic tests whether a coefficient of each independent variable significantly differs from zero, and the corresponding *p*-value determines if the null hypothesis can be rejected.

$$\ln WQ_{i,t} = \beta_1 \overline{\text{Temp}}_{i,t} + \beta_2 \overline{\text{Temp}}_{i,t}^2 + \beta_3 \overline{\text{Temp}}_{i,t} \times \text{Prec}_{i,t} + \eta_1 \text{GDP}_{i,t} + \eta_2 \text{Industry}_{i,t} + \eta_3 \text{Emission}_{i,t} + \eta_4 \text{Prec}_{i,t} + \alpha_i + \gamma_t + \varepsilon_{i,t} \quad (1)$$

where WQ_{i,t} represents the concentrations of water quality indicators (mg/L) of city *i* on day *t*, including DO, COD_{Mn}, and NH₃-N. Temp_{i,t} is the average temperature value (°C) of city *i* on day *t*. GDP_{i,t}, Industry_{i,t}, and Emission_{i,t} represent the total GDP, secondary sector output share, and amount of wastewater discharge of city *i* on day *t* in the corresponding year,

respectively. Prec_{i,t} indicates the total precipitation (m) of *i* on day *t*. α_i and γ_t are used as regional and daily fixed effects, respectively. $\varepsilon_{i,t}$ is the city-time error. Standard errors are clustered in cities.

In addition, we perform spatial spillover effects of water quality indicators, regional and seasonal heterogeneity analyses, as well as robustness tests, as described in the Supplementary Notes 5–7.

Empirical modeling of extreme temperatures

Given that temperature-related extreme event scenarios, such as high temperature and heatwaves, can cause more complex system responses in river water bodies^{9,66}, we screen out the samples for separate analysis. We define single-day high temperature as the maximum temperature Temp_{Max35} of city *i* exceeding 35 °C on day *t*, and this threshold has been adopted widely in previous studies^{67–69}. We construct and compare multiple models (Supplementary Note 8), and ultimately the model specification for single-day high temperature is shown in Eq. (2).

$$\begin{aligned} \ln WQ_{i,t} = & \beta_1 \text{Temp}_{\text{Max35}i,t} + \beta_2 \text{Temp}_{\text{Max35}i,t}^2 \\ & + \beta_3 \text{Temp}_{\text{Max35}i,t} \times \text{Fertilizer}_{i,t} + \eta_1 \text{GDP}_{i,t} + \eta_2 \text{Fertilizer}_{i,t} \\ & + \eta_3 \text{Agriculture}_{i,t} + \eta_4 \text{Industry}_{i,t} + \eta_5 \text{Pipe}_{i,t} + \alpha_i + \gamma_t + \varepsilon_{i,t} \end{aligned} \quad (2)$$

where Fertilizer_{i,t}, Agriculture_{i,t} and Pipe_{i,t} represent the amount of nitrogen fertilizer applied, primary sector output share, and drainage pipe length of city *i* on day *t* in the corresponding year, respectively.

We further investigate the impacts of heatwave events on water quality, which represent a prolonged period of hot weather, spanning several days to weeks⁷⁰. A heat wave involves both the intensity and persistence of high temperatures, and is therefore defined as in which the daily maximum temperature in a city *i* exceeds 35 °C for two, three, or four consecutive days^{67,71}. Thus, the heat wave variable Heatwave_{i,t} is set as a binary variable, equal to 1 if the above definition is met and 0 otherwise (see Eq. (3)). Heatwave_{i,t} is added to the single-day high temperature model, as shown in Eq. (3).

$$\begin{aligned} \ln WQ_{i,t} = & \beta_1 \text{Heatwave}_{i,t} + \eta_1 \text{Temp}_{\text{Max35}i,t} + \eta_2 \text{Temp}_{\text{Max35}i,t}^2 \\ & + \eta_3 \text{Temp}_{\text{Max35}i,t} \times \text{Fertilizer}_{i,t} + \eta_4 \text{GDP}_{i,t} + \eta_5 \text{Fertilizer}_{i,t} \\ & + \eta_6 \text{Agriculture}_{i,t} + \eta_7 \text{Industry}_{i,t} + \eta_8 \text{Pipe}_{i,t} + \alpha_i + \gamma_t + \varepsilon_{i,t} \end{aligned} \quad (3)$$

Quality-based water scarcity risk calculation

Water quality requirements depend on the intended use⁷², and therefore variations in water quality in a watershed can affect regional water use in the agricultural, industrial, and domestic sectors². Specific city water quality requirements are described in Supplementary Note 1. Quality-based water scarcity risk is calculated as the ratio of the amount of water required for dilution to achieve adequate water quality to the amount of water available for use², as shown in Eqs. (4) and (5). To capture the contribution of temperature to quality-based water scarcity risk, we further calculate the total effect of temperature on concentration contribution, as shown in Eq. (6).

$$dq_j = \begin{cases} \left(\frac{D_j * C_a}{C_{\max_{aj}}} - D_j \right)^0, & C_a \leq C_{\max_{aj}} \\ \left(\frac{D_j * C_a}{C_{\max_{aj}}} - D_j \right), & C_a > C_{\max_{aj}} \end{cases} \quad (4)$$

$$\text{WS}_{\text{quality}} = \frac{\sum_j dq_j}{Q - \text{EFR}} \quad (5)$$

$$\text{WS}_{\text{temp}} = \frac{C_{\text{temp},a}}{C_a} \times \text{WS}_{\text{quality}} \quad (6)$$

where dq_j represents the additional amount of dilution required by sector *j* to obtain acceptable water quality, and D_j is the amount of water withdrawn of sector *j*. C_a is the actual concentration level of water quality parameter *a*. C_{max_{aj}} indicates the maximum threshold value of the water-using sector *j* of parameter *a*. WS_{quality} is quality-based water scarcity, and Q is the total water resources of city *i*, including surface runoff and precipitation

infiltration recharge. EFR is the Environmental Flow Requirement, which is defined as 80% of the water availability according to the previous study². The remaining 20% can be considered blue water available for human use without compromising the integrity of water-dependent ecosystems and livelihoods downstream. $Q - EFR$ represents the amount of available water withdrawals for a city. WS_{temp} and $C_{temp,a}$ indicate the contribution of temperature to $WS_{quality}$ and the concentration of parameter a .

Reporting summary

Further information on research design is available in the Nature Portfolio Reporting Summary linked to this article.

Data availability

The source data supporting the findings of this study are available in Figshare at <https://doi.org/10.6084/m9.figshare.30415489.v1>.

Received: 13 May 2025; Accepted: 31 October 2025;

Published online: 17 December 2025

References

- Li, J. L. et al. Quality matters: pollution exacerbates water scarcity and sectoral output risks in China. *Water Res.* **224**, 9 (2022).
- Ma, T. et al. Pollution exacerbates China's water scarcity and its regional inequality. *Nat. Commun.* **11**, 9 (2020).
- van Vliet, M. T. H. et al. Global water scarcity including surface water quality and expansions of clean water technologies. *Environ. Res. Lett.* **16**, 12 (2021).
- Krueger, E., Rao, P. S. C. & Borchardt, D. Quantifying urban water supply security under global change. *Glob. Environ. Change-Hum. Policy Dimens.* **56**, 66–74 (2019).
- McDonald, R. I. et al. Urban growth, climate change, and freshwater availability. *Proc. Natl. Acad. Sci. USA* **108**, 6312–6317 (2011).
- Flörke, M., Schneider, C. & McDonald, R. I. Water competition between cities and agriculture driven by climate change and urban growth. *Nat. Sustain.* **1**, 51–58 (2018).
- He, C. Y. et al. Future global urban water scarcity and potential solutions. *Nat. Commun.* **12**, 11 (2021).
- Miller, J. D. & Hutchins, M. The impacts of urbanisation and climate change on urban flooding and urban water quality: A review of the evidence concerning the United Kingdom. *J. Hydrol. Reg. Stud.* **12**, 345–362 (2017).
- Van Vliet, M. T. H. et al. Global river water quality under climate change and hydroclimatic extremes. *Nat. Rev. Earth Environ.* **4**, 687–702 (2023).
- AghaKouchak, A. et al. in *Annual Review of Earth and Planetary Sciences*, Vol. 48, (eds R. Jeanloz & K. H. Freeman) 519–548 (Annual Reviews, 2020).
- Pörtner, H.-O. et al. *IPCC 2022: Climate Change 2022: Impacts, Adaptation and Vulnerability: Working Group II Contribution to the Sixth Assessment Report of the Intergovernmental Panel on Climate Change* (Cambridge University Press, 2022).
- Mosley, L. M. Drought impacts on the water quality of freshwater systems: review and integration. *Earth-Sci. Rev.* **140**, 203–214 (2015).
- Li, L. et al. River water quality shaped by land-river connectivity in a changing climate. *Nat. Clim. Change*, **13**, <https://doi.org/10.1038/s41558-023-01923-x> (2024).
- Graham, D. J., Bierkens, M. F. P. & van Vliet, M. T. H. Impacts of droughts and heatwaves on river water quality worldwide. *J. Hydrol.* **629**, 13 (2024).
- Wang, X. P. et al. A holistic assessment of spatiotemporal variation, driving factors, and risks influencing river water quality in the northeastern Qinghai-Tibet Plateau. *Sci. Total Environ.* **851**, 12 (2022).
- Han, Y. L. & Bu, H. M. The impact of climate change on the water quality of Baiyangdian Lake (China) in the past 30 years (1991–2020). *Sci. Total Environ.* **870**, 9 (2023).
- Jane, S. F. et al. Widespread deoxygenation of temperate lakes. *Nature* **594**, 66 (2021).
- Zhi, W., Klingler, C., Liu, J. T. & Li, L. Widespread deoxygenation in warming rivers. *Nat. Clim. Change*, **28**, <https://doi.org/10.1038/s41558-023-01793-3> (2023).
- Kellerman, A. M., Dittmar, T., Kothawala, D. N. & Tranvik, L. J. Chemodiversity of dissolved organic matter in lakes driven by climate and hydrology. *Nat. Commun.* **5**, 8 (2014).
- Chen, B. et al. In search of key: protecting human health and the ecosystem from water pollution in China. *J. Clean. Prod.* **228**, 101–111 (2019).
- Guan, D. B. et al. Lifting China's water spell. *Environ. Sci. Technol.* **48**, 11048–11056 (2014).
- Vörösmarty, C. J. et al. Global threats to human water security and river biodiversity. *Nature* **467**, 555–561 (2010).
- Lu, Y. L. et al. Impacts of soil and water pollution on food safety and health risks in China. *Environ. Int.* **77**, 5–15 (2015).
- Zhang, H. X. et al. Changes in China's river water quality since 1980: management implications from sustainable development. *npj Clean. Water* **6**, 10 (2023).
- Zhang, H. R. et al. Natural and anthropogenic imprints on seasonal river water quality trends across China. *npj Clean. Water* **8**, 13 (2025).
- Sun, Y. et al. Understanding human influence on climate change in China. *Natl. Sci. Rev.* **9**, 16 (2022).
- Li, R. Y., Xiao, X., Zhao, Y., Tu, B. H. & Zhang, Y. M. Screening of efficient ammonia-nitrogen degrading bacteria and its application in livestock wastewater. *Biomass Convers. Biorefin.* **14**, 8513–8521 (2024).
- Wang, H. Y., Zou, Z. C., Chen, D. & Yang, K. Effects of temperature on aerobic denitrification in a bio-ceramsite reactor. *Energy Sources Part A Recovery Util. Environ. Eff.* **38**, 3236–3241 (2016).
- Collins, S. M. et al. Winter precipitation and summer temperature predict lake water quality at macroscales. *Water Resour. Res.* **55**, 2708–2721 (2019).
- Rao, K. et al. Interactive effects of environmental factors on phytoplankton communities and benthic nutrient interactions in a shallow lake and adjoining rivers in China. *Sci. Total Environ.* **619**, 1661–1672 (2018).
- Tong, H. H., Yin, K., Giannis, A., Ge, L. Y. & Wang, J. Y. Influence of temperature on carbon and nitrogen dynamics during in situ aeration of aged waste in simulated landfill bioreactors. *Bioresour. Technol.* **192**, 149–156 (2015).
- Chen, X. P. et al. Producing more grain with lower environmental costs. *Nature* **514**, 486 (2014).
- Yvon-Durocher, G., Jones, J. I., Trimmer, M., Woodward, G. & Montoya, J. M. Warming alters the metabolic balance of ecosystems. *Philos. Trans. R. Soc. B Biol. Sci.* **365**, 2117–2126 (2010).
- Hoang, H. G. et al. The nitrogen cycle and mitigation strategies for nitrogen loss during organic waste composting: a review. *Chemosphere* **300**, 15 (2022).
- Peng, K., Qin, B. Q., Cai, Y. J., Gong, Z. J. & Jeppesen, E. Water column nutrient concentrations are related to excretion by benthic invertebrates in Lake Taihu, China. *Environ. Pollut.* **261**, 9 (2020).
- Rahimi, S., Modin, O. & Mijakovic, I. Technologies for biological removal and recovery of nitrogen from wastewater. *Biotechnol. Adv.* **43**, 25 (2020).
- Hanson, P. C., Carpenter, S. R., Armstrong, D. E., Stanley, E. H. & Kratz, T. K. Lake dissolved inorganic carbon and dissolved oxygen: changing drivers from days to decades. *Ecol. Monogr.* **76**, 343–363 (2006).
- Obertegger, U., Pindo, M. & Flaim, G. Multifaceted aspects of synchrony between freshwater prokaryotes and protists. *Mol. Ecol.* **28**, 4500–4512 (2019).
- Tiquia, S. M. Metabolic diversity of the heterotrophic microorganisms and potential link to pollution of the Rouge River. *Environ. Pollut.* **158**, 1435–1443 (2010).
- Sánchez-España, J. et al. Anthropogenic and climatic factors enhancing hypolimnetic anoxia in a temperate mountain lake. *J. Hydrol.* **555**, 832–850 (2017).

41. Liu, Y. Y. et al. Effect of water chemistry and hydrodynamics on nitrogen transformation activity and microbial community functional potential in hyporheic zone sediment columns. *Environ. Sci. Technol.* **51**, 4877–4886 (2017).

42. Cahoon, L. B. & Hanke, M. H. Inflow and infiltration in coastal wastewater collection systems: effects of rainfall, temperature, and sea level. *Water Environ. Res.* **91**, 322–331 (2019).

43. Zanon, J. A., Favaretto, N., Goularte, G. D., Dieckow, J. & Barth, G. Manure application at long-term in no-till: effects on runoff, sediment and nutrients losses in high rainfall events. *Agric. Water Manag.* **228**, 105908 (2020).

44. Sinha, E., Michalak, A. M. & Balaji, V. Eutrophication will increase during the 21st century as a result of precipitation changes. *Science* **357**, 405–408 (2017).

45. Liang, L., Ma, L., Liu, T., Sun, B. & Zhou, Y. Spatiotemporal variation of the temperature mutation and warming hiatus over northern China during 1951–2014. *China Environ. Sci.* **38**, 1601–1615 (2018).

46. Liu, D. et al. Changes in riverine organic carbon input to the ocean from mainland China over the past 60 years. *Environ. Int.* **134**, 14 (2020).

47. Hall, R. O. & Ulseth, A. J. Gas exchange in streams and rivers. *Wiley Interdiscip. Rev. Water* **7**, 18 (2020).

48. Aleksandrov, S. V. Biological production and eutrophication of Baltic Sea estuarine ecosystems: the Curonian and Vistula Lagoons. *Mar. Pollut. Bull.* **61**, 205–210 (2010).

49. Jonsson, M., Polvi, L. E., Sponseller, R. A. & Stenroth, K. Catchment properties predict autochthony in stream filter feeders. *Hydrobiologia* **815**, 83–95 (2018).

50. Hrdinka, T., Vlasák, P., Havel, L. & Mlejnská, E. Possible impacts of climate change on water quality in streams of the Czech Republic. *Hydrolog. Sci. J.* **60**, 192–201 (2015).

51. Xiao, X. Y., Fu, J. J. & Yu, X. Impacts of extreme weather on microbiological risks of drinking water in coastal cities: a review. *Curr. Pollut. Rep.* **9**, 259–271 (2023).

52. Scafaro, A. P. et al. Responses of leaf respiration to heatwaves. *Plant Cell Environ.* **44**, 2090–2101 (2021).

53. He, G. X. et al. Assessing the impact of atmospheric heatwaves on intertidal clams. *Sci. Total Environ.* **841**, 10 (2022).

54. Qiao, X. L., Chen, C. X. & Zhang, Z. J. Comparative study of nitrification performances of immobilized cell fluidized bed reactor and contact oxidation biofilm reactor in treating high strength ammonia wastewater. *J. Chem. Technol. Biotechnol.* **83**, 84–90 (2008).

55. Kumari, M., Tripathi, S., Pathak, V. & Tripathi, B. Chemometric characterization of river water quality. *Environ. Monit. Assess.* **185**, 3081–3092 (2013).

56. Lee, J., Lee, S., Yu, S. & Rhew, D. Relationships between water quality parameters in rivers and lakes: BOD5, COD, NBOPs, and TOC. *Environ. Monit. Assess.* **188**, 8 (2016).

57. Ha, D. W. et al. Long-term water quality fluctuations in the Seomjin river system determined using LOWESS and seasonal Kendall analyses. *Water Air Soil Pollut.* **233**, 15 (2022).

58. Hersbach, H. et al. ERA5 hourly data on single levels from 1940 to present. *Copernicus Clim. Change Serv. (C3S) Clim. Data Store (CDS)* **10**, 10.24381 (2023).

59. Donat, M. G., Lowry, A. L., Alexander, L. V., O’Gorman, P. A. & Maher, N. More extreme precipitation in the world’s dry and wet regions. *Nat. Clim. Chang.* **6**, 508 (2016).

60. Lv, Z. Q., Xiao, X. L., Wang, Y., Zhang, Y. & Jiao, N. Z. Improved water quality monitoring indicators may increase carbon storage in the oceans. *Environ. Res.* **206**, 9 (2022).

61. Huang, J. C. et al. Characterizing the river water quality in China: recent progress and on-going challenges. *Water Res.* **201**, 14 (2021).

62. Ministry of Ecological and Environment of the People’s Republic of China. *Technical Regulation for Urban Surface Water Environmental Quality Ranking (Trial)*. (General Office of the Ministry of Environmental Protection, 2017).

63. Sinha, E. & Michalak, A. M. Precipitation dominates interannual variability of riverine nitrogen loading across the continental United States. *Environ. Sci. Technol.* **50**, 12874–12884 (2016).

64. Kotz, M., Wenz, L., Stechemesser, A., Kalkuhl, M. & Levermann, A. Day-to-day temperature variability reduces economic growth. *Nat. Clim. Change* **11**, 319–U354 (2021).

65. Weng, Z. X., Liu, T. T., Wu, Y. F. & Cheng, C. Y. Air quality improvement effect and future contributions of carbon trading pilot programs in China. *Energy Policy* **170**, 12 (2022).

66. Dietrich, J. S., Welti, E. A. R. & Haase, P. Extreme climatic events alter the aquatic insect community in a pristine German stream. *Clim. Change* **176**, 16 (2023).

67. Coppola, E. et al. Climate hazard indices projections based on CORDEX-CORE, CMIP5 and CMIP6 ensemble. *Clim. Dyn.* **57**, 1293–1383 (2021).

68. Farah, S., Whaley, D., Saman, W. & Boland, J. Integrating climate change into meteorological weather data for building energy simulation. *Energy Build.* **183**, 749–760 (2019).

69. China Meteorological Administration. *Monitoring indices of high temperature extremes*. (China Meteorological Administration, 2015).

70. Shi, Z. T., Jia, G. S., Zhou, Y. Y., Xu, X. Y. & Jiang, Y. Amplified intensity and duration of heatwaves by concurrent droughts in China. *Atmos. Res.* **261**, 9 (2021).

71. Cheng, B.-J. et al. Short-term effects of heatwaves on clinical and subclinical cardiovascular indicators in Chinese adults: a distributed lag analysis. *Environ. Int.* **183**, 108358 (2024).

72. van Vliet, M. T. H., Flörke, M. & Wada, Y. Quality matters for water scarcity. *Nat. Geosci.* **10**, 800–802 (2017).

Acknowledgements

This work was supported by the National Key Research and Development Program of China (2023YFC3205703) and the National Natural Science Foundation of China (52170189, 72488101, and 72234003).

Author contributions

Kehan Liang: Methodology, Software, Validation, Formal analysis, Data process, Writing - original draft, Visualization. Litiao Hu: Methodology, Software, Validation, Formal analysis, Data process, Writing - original draft, Visualization. Zongwei Ma: Conceptualization, Methodology, Writing - review & editing, Supervision, Project administration, Funding acquisition. Shenyuan Huang: Conceptualization, Methodology. Miaomiao Liu: Conceptualization, review & editing. Wen Fang: Conceptualization, review & editing. Jianxun Yang: Conceptualization, review & editing. Jun Bi: Methodology, Writing - review & editing, Funding acquisition.

Competing interests

The authors declare no competing interests.

Additional information

Supplementary information The online version contains supplementary material available at <https://doi.org/10.1038/s43247-025-02978-8>.

Correspondence and requests for materials should be addressed to Zongwei Ma.

Peer review information *Communications Earth and Environment* thanks the anonymous reviewers for their contribution to the peer review of this work. Primary Handling Editors: Mengru Wang, Somaparna Ghosh.

Reprints and permissions information is available at <http://www.nature.com/reprints>

Publisher’s note Springer Nature remains neutral with regard to jurisdictional claims in published maps and institutional affiliations.

Open Access This article is licensed under a Creative Commons Attribution-NonCommercial-NoDerivatives 4.0 International License, which permits any non-commercial use, sharing, distribution and reproduction in any medium or format, as long as you give appropriate credit to the original author(s) and the source, provide a link to the Creative Commons licence, and indicate if you modified the licensed material. You do not have permission under this licence to share adapted material derived from this article or parts of it. The images or other third party material in this article are included in the article's Creative Commons licence, unless indicated otherwise in a credit line to the material. If material is not included in the article's Creative Commons licence and your intended use is not permitted by statutory regulation or exceeds the permitted use, you will need to obtain permission directly from the copyright holder. To view a copy of this licence, visit <http://creativecommons.org/licenses/by-nc-nd/4.0/>.

© The Author(s) 2025